

Dynamics of deep sea surface buoy system for ocean mixed layer experiment

W. KOTERAYAMA*, S. MIZUNO**, K. MARUBAYASHI*
and M. ISHIBASHI*

Abstract: A deep sea surface buoy system for measuring the water temperature and current velocity in the upper mixed layer has been developed. On-site, long-term experiments were carried out at 29°N, 133°E, south of Japan in the Pacific Ocean from 1987 to 1991, and provided useful data in the study of heat and momentum transfer between the ocean and the atmosphere. To evaluate the accuracy of the measurements and improve the data quality, motions of the surface buoy and instruments fixed to the mooring line were analyzed by numerical simulation.

1. Introduction

Studies of ocean-atmosphere coupling require knowledge of the water temperature and current velocity. This necessitates long-term observation, and until the artificial satellite system has a device for underwater measurements, the moored buoy offers the best measuring method to study an ocean mixed layer. The area of ocean mixed layer experiments (OMLET) must be far remote from the land mass so that the effects of land on the data are eliminated. Sea depth at such a location is usually between 3000m and 5000m. The buoy system should be light and small in size so that researchers can handle it by themselves; it is important for them to continue the study for a long time under the restricted economical condition. In this report the dynamics of a comparatively small surface buoy system moored in mid-ocean at a depth of 5000m is reported, and the effects of the motions of the system on the accuracy of the data obtained are discussed.

2. Design of the buoy system

Since the authors previously reported details of the method of calculating the dynamics of the surface buoy system (KOTERAYAMA *et al.*, 1986), the design scheme is explained here briefly. The

environmental conditions must first be determined. The sea area for the experiment was decided as 29°N, 133°E. Water depth is about 5000m. The maximum values of wave height and wind velocity used in designing an ocean structure to be moored in mid-ocean are generally 30m and 50m/s respectively. These were values used in our design. The system had to be safe under these conditions (survival condition). The wind load acting on a small surface buoy directly is minimal and negligible, but the drag force due to the surface current induced by wind must be considered in the calculation. The magnitude of the wind induced surface current was estimated by assuming Ekman drift current (EKMAN, 1905). The wave-making force can be neglected compared with the viscous drag force because the wave length is much larger than the diameter of the surface buoy. The effects of the ocean current are dominant on deep sea mooring because the line is very long. In this study the highest value of the current profile proposed by Woods Hole Oceanographic Institution was adopted (Fig. 1; CLAY, 1983) for the design of the system. The force due to current acts on the mooring line as a drag force. The Lumped Mass Method used to estimate the data accuracy is explained here briefly.

As shown in the concept of the Lumped Mass Method (Fig. 2), the cable is modeled as N-discrete masses interconnected by springs of which the spring-constants are equal to those of

* Research Institute for Applied Mechanics, Kyushu University, Kasuga, 816 Japan

**Department of Civil Engineering Hiroshima Institute of Technology, Hiroshima, 731-51 Japan

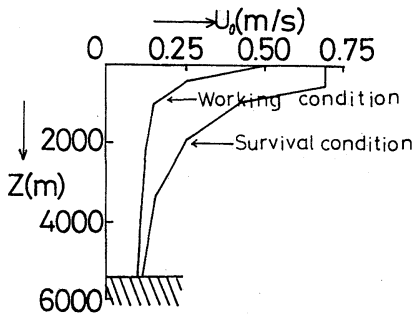


Fig. 1. Vertical velocity profiles of ocean current used for buoy design.

the mooring rope. All force such as the drag force, the added mass force, the inertia force, the buoyancy and weight acting on the cable are considered to be concentrated on each mass, so that the motions of the cable can be represented by simultaneous differential equations. The point of lumped masses in the calculation model is selected to coincide with the massive points in the real system; buoy, floats, current meters, which enables us to get a realistic model. In this study two-dimensional numerical simulations are adopted, so that the motion of each mass is described by two simultaneous equations. Finally, the motions of N-lumped masses can be written by 2N-simultaneous equations. These equations cannot be solved analytically but numerically because they include strong nonlinear terms.

Fig. 3 shows a schematic view of the buoy system which was designed on the basis of these numerical simulations and improved through on-site experiments. Since most accidents with the surface buoy system such as the severance of the mooring line occur near the buoy, the floats were distributed in such a way that the entire system except the surface buoy is retrievable through the buoyancy of the floats and activation of the acoustic release even if the surface buoy is lost. Under extremely severe conditions the line tension becomes very great. The surface buoy is pulled down to the subsurface when the tension becomes greater than the excess buoyancy of the surface buoy. To prevent this the surface buoy must be very large, which is not practical. The maximum value of the line tension nearly equals the smaller value of the sinker

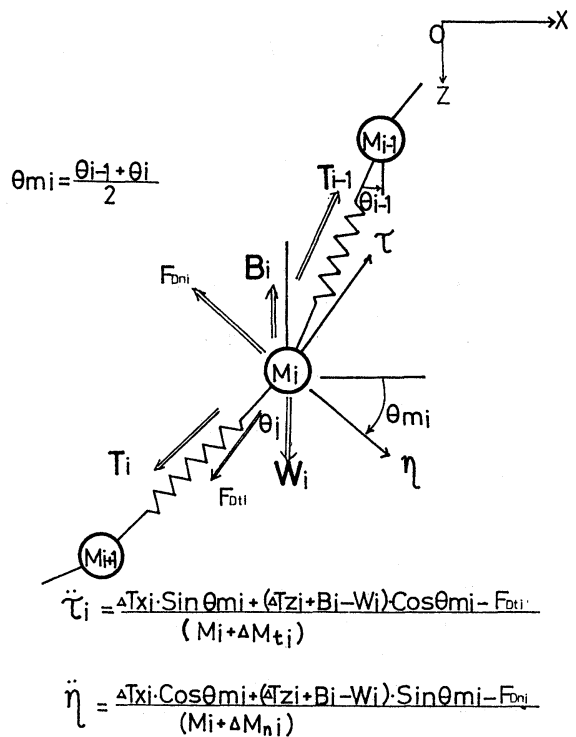


Fig. 2. Concept of Lumped Mass Method.

weight in water and the excess buoyancy of the surface buoy. The sinker is raised when the vertical component of the line tension becomes greater than its weight. The line tension does not become much greater than the weight of the sinker. We had to decide to make the surface buoy submerge or the sinker to be raised under severe conditions in order to avoid making the system very large. We finally selected a light sinker weighing less than the excess buoyancy of the surface buoy, because otherwise the buoy must be very strong to endure the water pressure. We anticipated that the sinker would lift and the entire system would drift under severe conditions. To compensate for this eventuality we installed a satellite positioning system (ARGOS SYSTEM) to locate the system when it moved from the initial point. For safety, floats should be positioned between the buoy and the depth of 1000m, but these floats increase the vertical displacement of the instrument and deteriorate data, so the floats concentrated at 1000m depth in the final design. The mooring

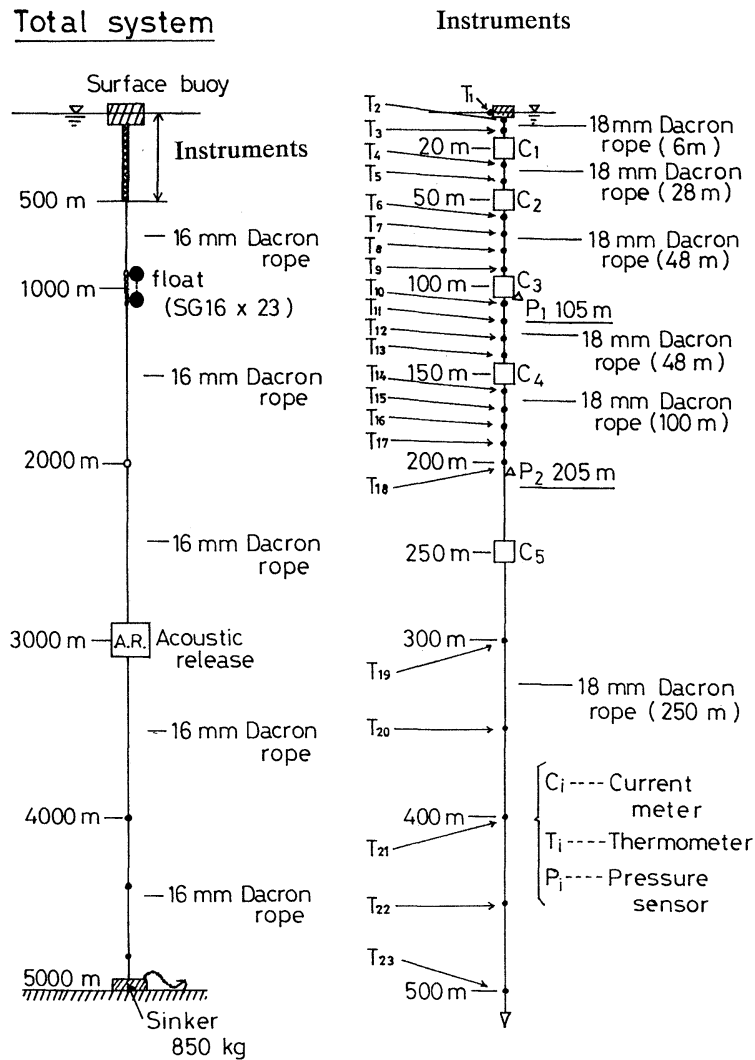


Fig. 3. Schematic view of buoy system designed for ocean mixed layer experiment.

line is of DACRON, because of its high strength and good chemical characteristics under the high pressure environment of the deep sea. The surface buoy is of rubber because of its toughness in potential collisions with ships, and its deployment and retrieval is fairly easy on the mother ship. The buoyancy of the surface buoy is 1500kg and its weight in air is 440kg.

Thus, we were able to design a light and compact buoy system for very deep sea experiment using accurate calculations for the buoy dynamics.

3. On-site experiments

This buoy system was used in on-site experiments carried out in 1987, 1988, 1989 and 1990. The results of the 1990 experiment are reported here. It was moored 133°16' E, 29°09' N by university ships; Keiten Maru of Kagoshima University, and recovered by Hakuho Maru of Tokyo University. Photo 1 shows scenes of the deployment. Difficult steps in this action would usually be the launching of the surface buoy and deployment of the sinker, because surface buoy is fragile and the sinker is heavy. However, those steps were fairly easy because the surface

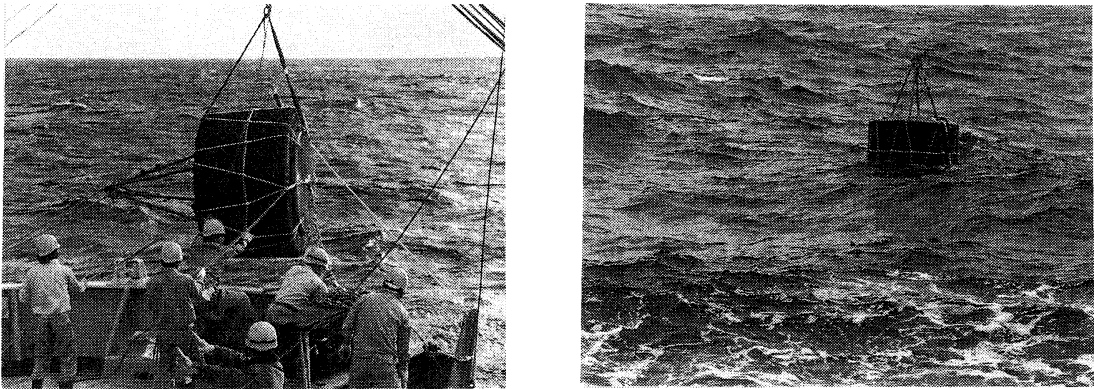


Photo. 1. Scenes of an experiment.

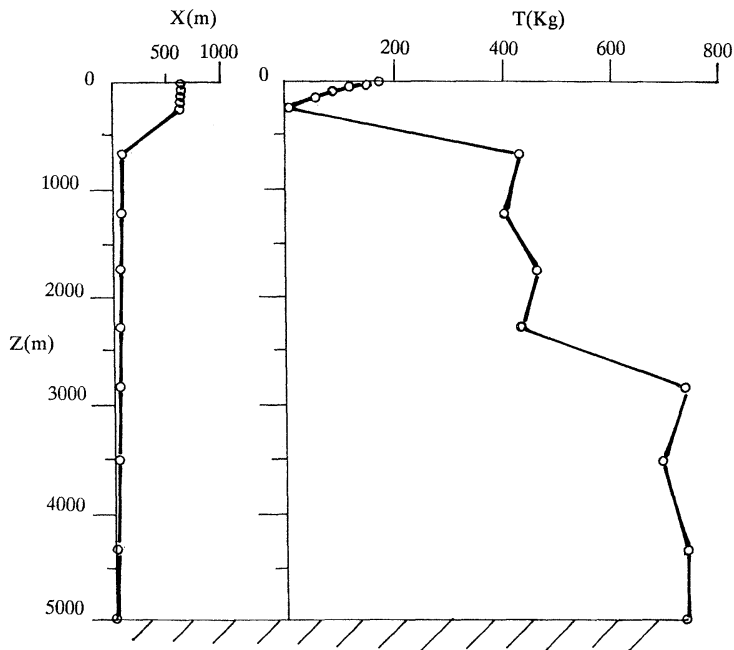


Fig. 4. Statical configuration of mooring line and tension distribution obtained by calculation.

buoy can withstand collisions or bumping and the sinker is comparatively light.

The statical configuration of the mooring line and tension distribution are shown in Fig. 4. The instruments are between the sea surface and 250m depth in order to collect data in the mixed layer, and the figure shows that the vertical displacements of the instruments are very small in this design. The current velocity used in the calculation is 0.1m/s (measured value) from 0 to 200m depth and 0.05m/s (estimated) below

200m. The current velocity is minimal in this case, so there is little statical tension. The shape of the statical configuration suggests that the spindle rod of the current meter C_s at 250m depth is subjected to not only the tension but the bending moment. The spindle rod of C_s was broken by its fatigue failure due to the action of the bending moment caused by waves and current so that the upper system including the surface buoy drifted though found with the help of the satellite positioning system. This weakness will be

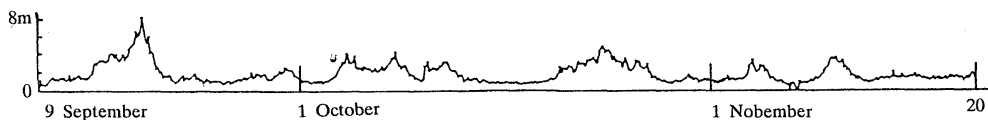


Fig. 5. Wave record by weather observation buoy of Meteorological Agency.

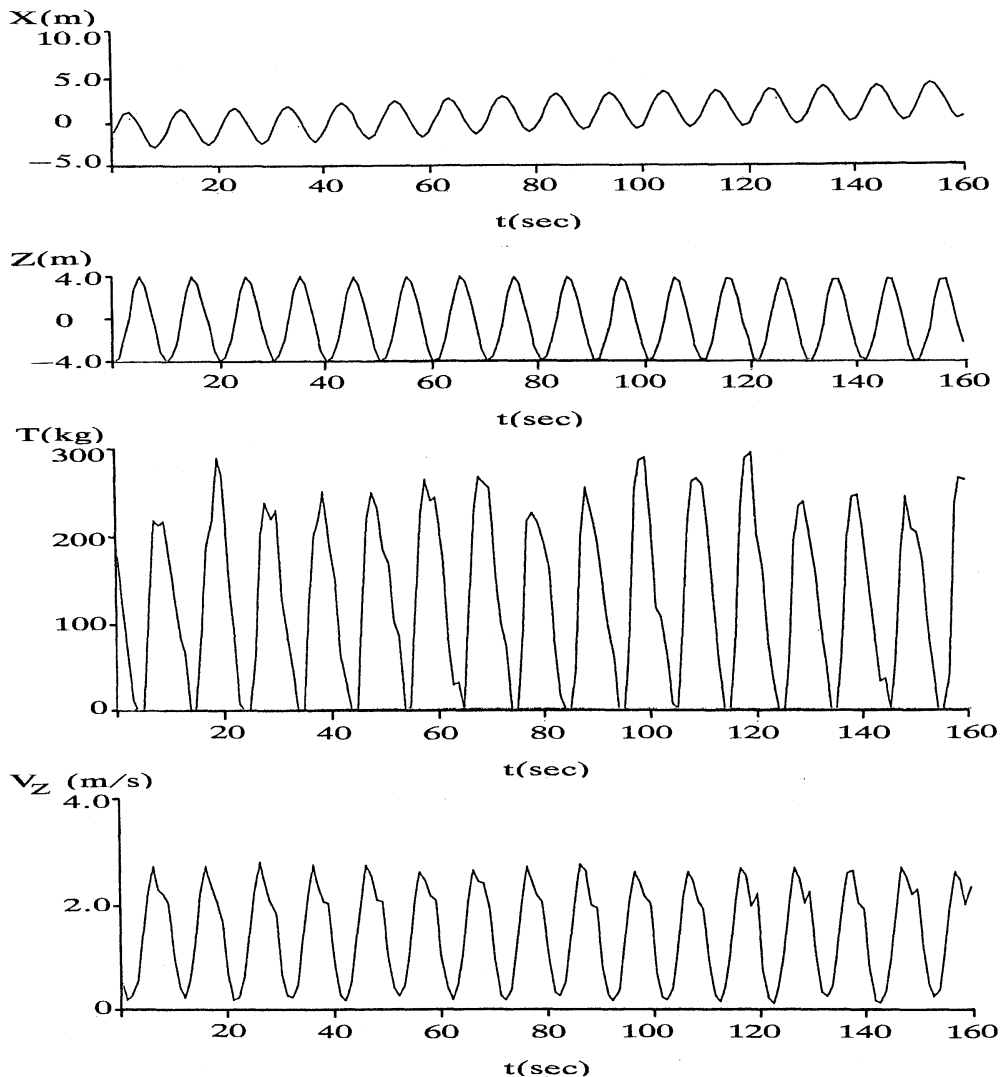


Fig. 6. Motions of surface buoy and dynamic tension of mooring line in waves ($H_w=8\text{m}$, $T_w=10\text{ sec}$).

improved by fixing a mass or drag just below the current meter.

The wave records shown in Fig. 5 were obtained with the weather observation buoy of the JAPAN Meteorological Agency located at 29°N , 135°E . The maximum wave height was 8m.

Quality of the current data obtained by the surface buoy system is generally believed not as good as that by the submerged buoy system because of the motion of the surface buoy induced by waves and surface currents. It is thus important to evaluate the motions of the instruments

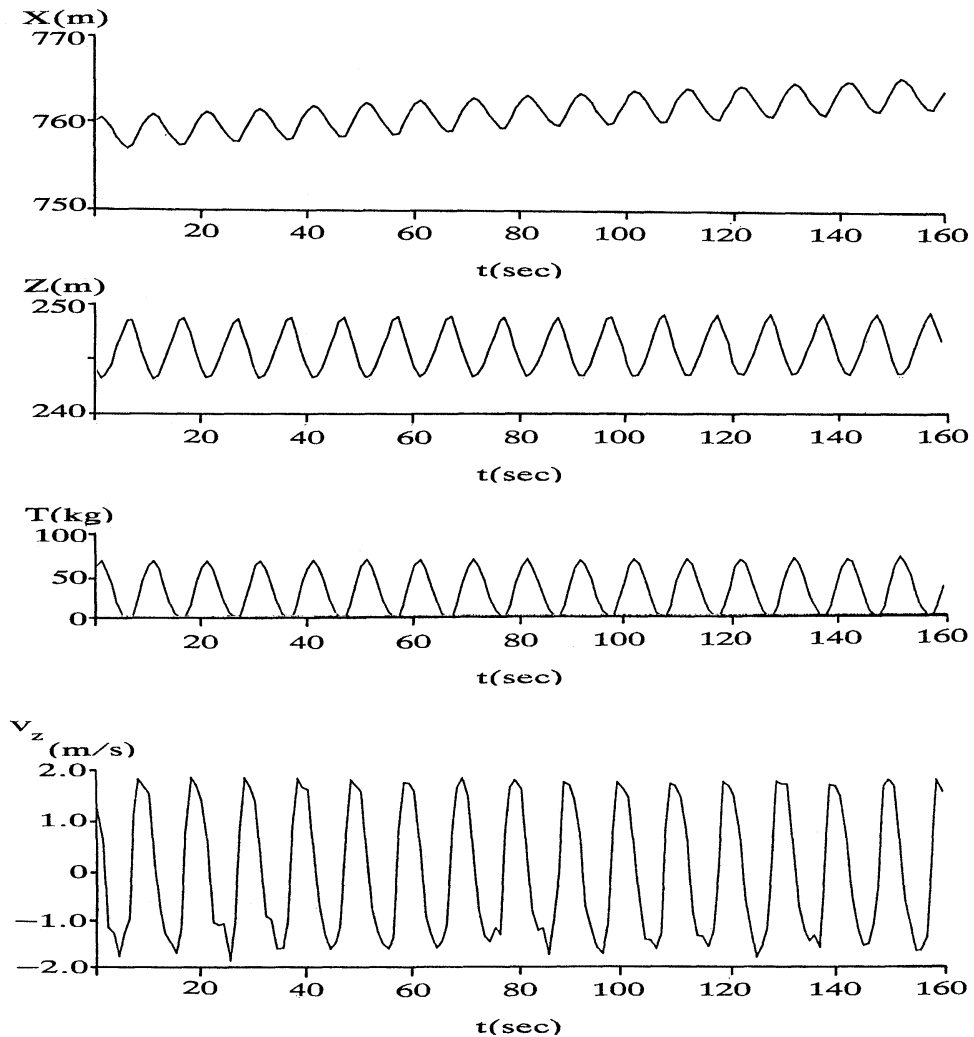


Fig. 7. Motions of C_s and dynamic tension of mooring line at C_s .

fixed to the mooring line.

Figure 6 shows calculation results of the motions of the surface buoy and dynamic tension of the mooring line for regular waves of 8m height and 10 sec period. The current is also taken into the consideration, but details of the current measurements will be explained later. From top to bottom in the figure are shown horizontal displacement X and vertical displacement Z of the surface buoy, line tension T at the surface buoy and the vertical velocity V_z of the surface buoy. The theory of floating body dynamics shows that the motion amplitudes of a small

body compared with wave length are almost the same as the wave amplitude when the restriction of the mooring line is not strong, which is confirmed by our calculations. The phase difference between the vertical displacement Z and wave surface is almost zero and the surface buoy follows the wave surface with fidelity. Under survival conditions such as current, wind and waves, the surface buoy occasionally submerges (KOTERAYAMA *et al.*, 1986). But it did not occur because of weak current. As the figure shows, the buoy drifts gradually from the initial point of the static balance, which is shown in Fig. 4.

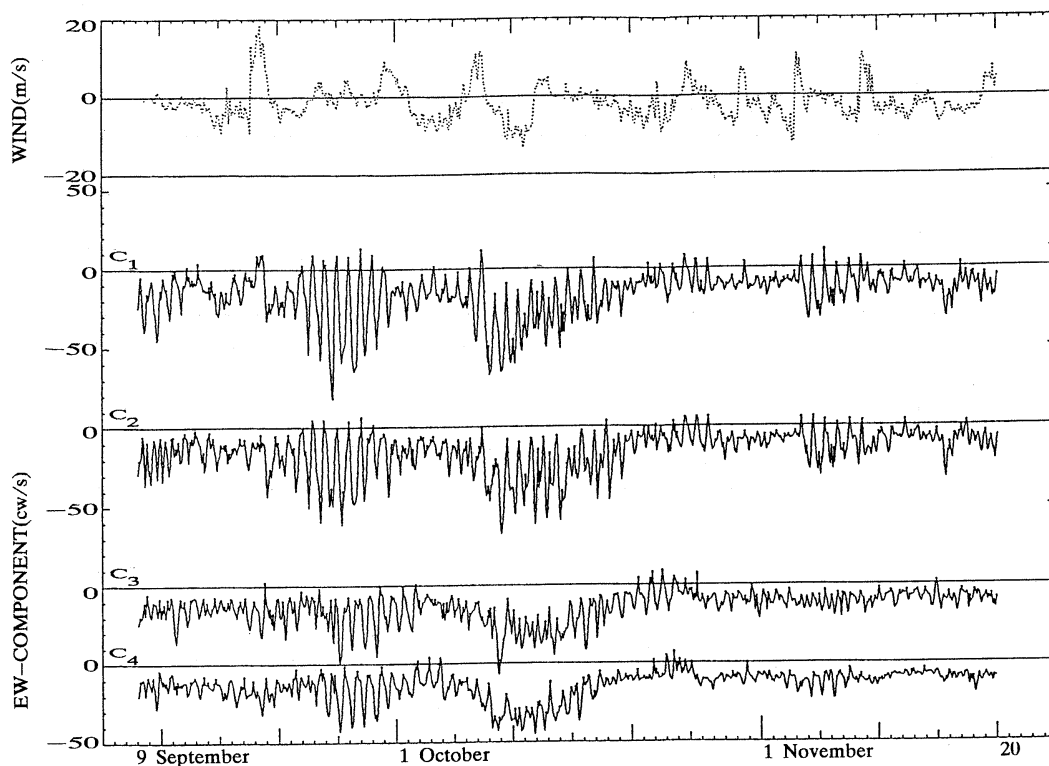


Fig. 8. Time series of wind velocity and current velocities measured with $C_1 \sim C_4$.

It is a result of the increase of the steady drag force generated by the interaction between waves and current, and a kind of transient motion. At a glance, the tension variation is irregular. The variation of phase difference between the waves and mooring line motions causes this irregularity and the variation may be a numerical error. The maximum tension is about 300kg, small enough as compared with the breaking tension of the mooring line (7 tons). It is undesirable from a safety standpoint that the tension becomes zero, which may kink the line. For this reason a wire rope was not used in this system. A kink is fatal for wire rope. Even a syntactic rope might cling to the instruments at zero tension. The zero tension occurs when the static tension of a line is smaller than the amplitude of dynamic tension. A large static tension is thus desirable, but requires that the surface buoy be large and is therefore contrary to the design philosophy.

The motions of the deepest current meter C_5

and the tension variation of the line at that point are shown in Fig. 7 using the coordinate system X and Z shown in Fig. 4. The motion amplitude is 3.7m horizontally and 5.6m vertically. The maximum tension is about 60 kg and the tension variation induced by waves is very small, but the vertical velocity V_z varies between -1.5m/s and 1.5m/s . The horizontal velocity of C_5 is estimated $1.0\text{m/s} \sim -1.0\text{m/s}$ from the amplitude of the displacement and its period. Under these conditions it is difficult to measure a small current velocity accurately with this type of the current meter (Savonius rotor with a vane) because the vane can not follow the direction change in high frequency velocity, and the oscillating component due to waves can not be measured properly. The steady component is affected by the error. The accuracy of current velocity measurement in a storm is therefore dubious. Another type of meter should be adopted if measurement of current velocity in a storm is desired.

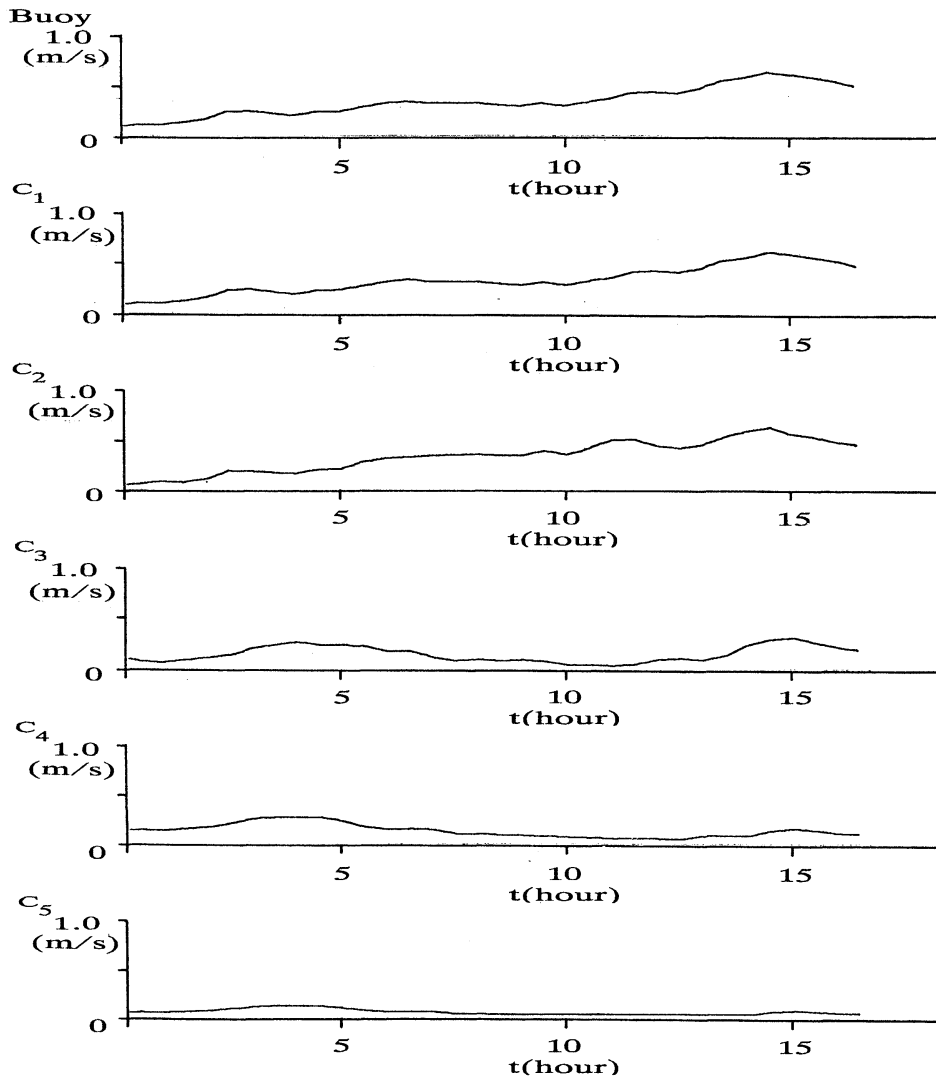


Fig. 9. Time series of current velocities used in calculation.

Fig. 8 shows the time series of the current velocity measured with C_1 to C_4 at the locations shown in Fig. 3. The current velocities oscillated violently during September 22–30, October 6–16, and November 3–9. The oceanographical discussion of these phenomena will appear in a later paper, and here the reliability of the measured data is investigated. We consider that the oscillations in the current record were not the result of buoy motion due to changes in wind velocity, because the wind data shown at the top of the figure (which was obtained by the weather

observation buoy of the Japan Meteorological Agency) does not reflect oscillations of the same frequency, and the natural frequency of the buoy system is much higher than that of the oscillation. We therefore guess that the oscillations must be those of current velocity. The recorded current velocity is that from the moving current meter, and the absolute velocity must be obtained by adding the horizontal velocity of the current meter induced by the current oscillation and mooring line motion. The motion of the buoy system is calculated for 16 hours from

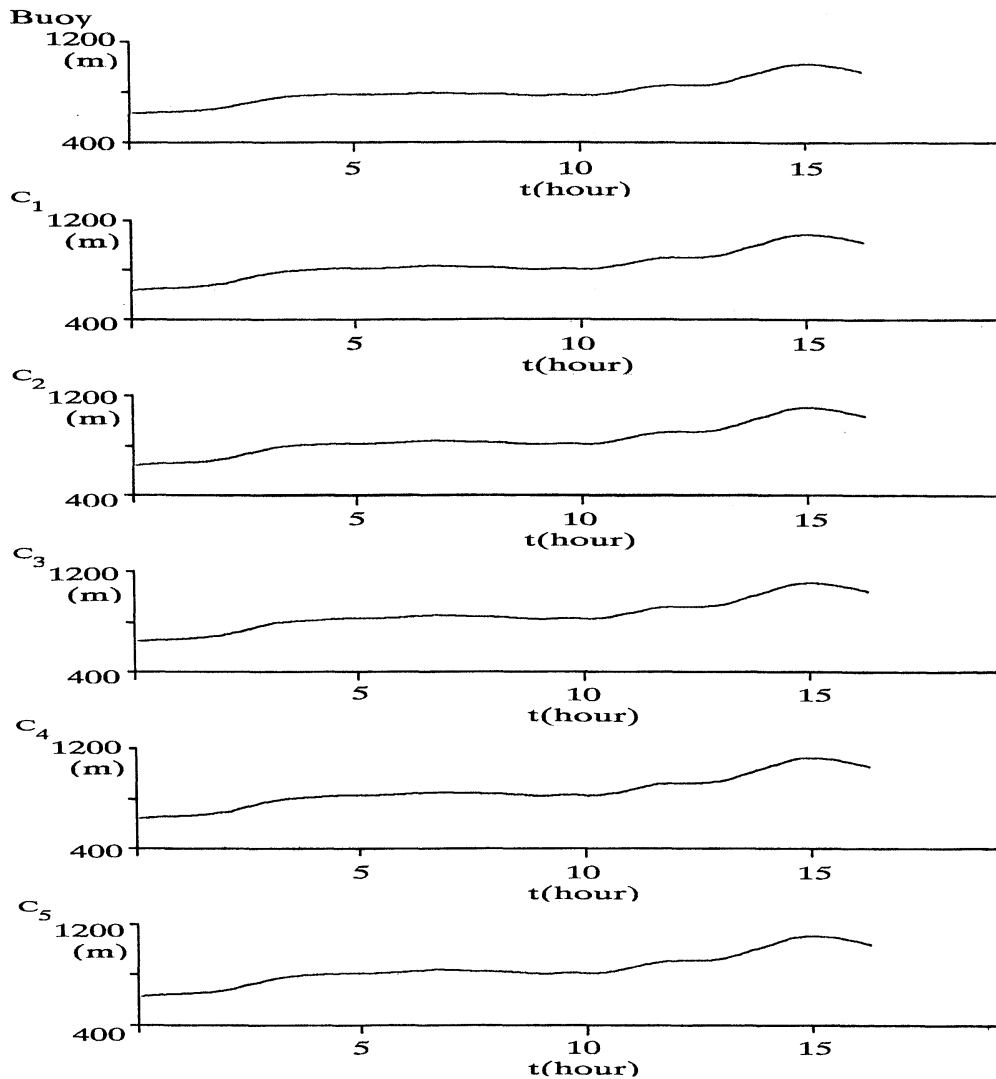


Fig. 10. Horizontal displacement of buoy and current meters obtained by calculation.

22:00 of September 23 to 14:00 of the next day when the current oscillation was strongest. The current velocities at each of the lumped masses used in the calculation are shown in Fig. 9. As a first approximation these absolute velocities are assumed to be equal to the relative ones measured by the current meters, where the current velocity at the surface buoy is assumed to be equal to that at C_1 , and all the other values are measured ones. The velocities at lumped masses deeper than C_5 are assumed to be 0.05 m/s.

The calculated horizontal displacement of each current meter is shown in Fig. 10, where the time lag of the motion from the current variation is about 30 minutes. This fact means that the system goes on moving for 30 minutes after the peak of the current. The maximum displacement of the surface buoy is 480 m and that of C_5 is 380 m.

Fig. 11 shows the horizontal motion velocity of each current meter. The maximum drifting velocities (3.6 cm/s) are those of the surface buoy and C_1 at 11:30 on September 24. The

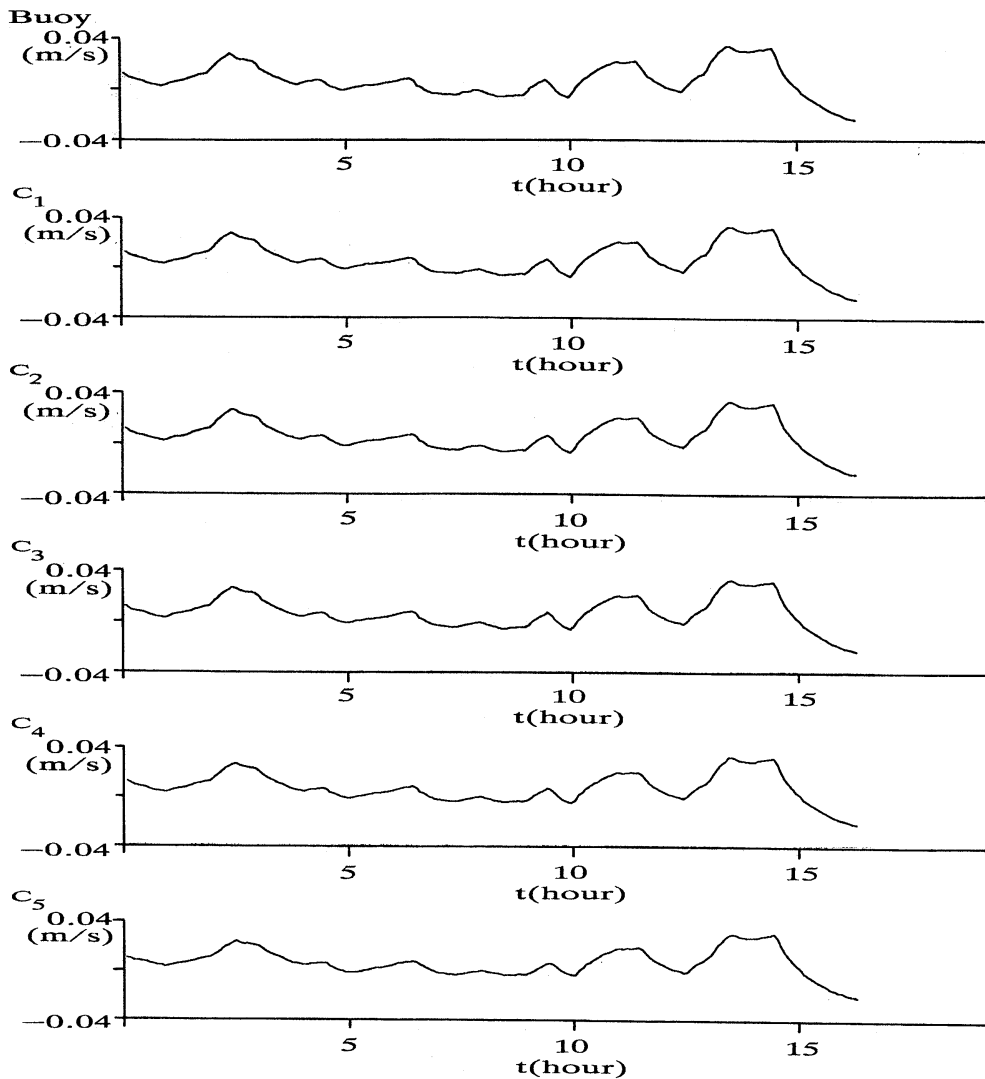


Fig. 11. Horizontal drifting velocities of current meters obtained by calculation.

maximum velocity was continued for one hour. After 12:30 when the maximum current velocity was recorded, their drifting velocities became vanishingly small. After 13:00 the drifting velocities became negative and the system began to return to original levels. The tendency of the drift of C_5 was the same as C_1 and finally the maximum drifting velocity throughout the entire system was estimated as 3.6 cm/s. Therefore, the drifting velocities of the current meters were less than 5.5% of the maximum current velocity of 65cm/s recorded by C_1 . We may

assume that this ratio does not vary remarkably with the current velocity. We can obtain the second approximation for the absolute velocity by adding the drifting velocities to those recorded by the current meters, and through the iterative procedure, can obtain higher approximate values. This iteration procedure is convergent when it is a linear system or the ratio does not increase suddenly. In case the mooring system has a resonant frequency in the horizontal motion, the ratio increases suddenly at the resonant frequency and the iteration might be divergent, but

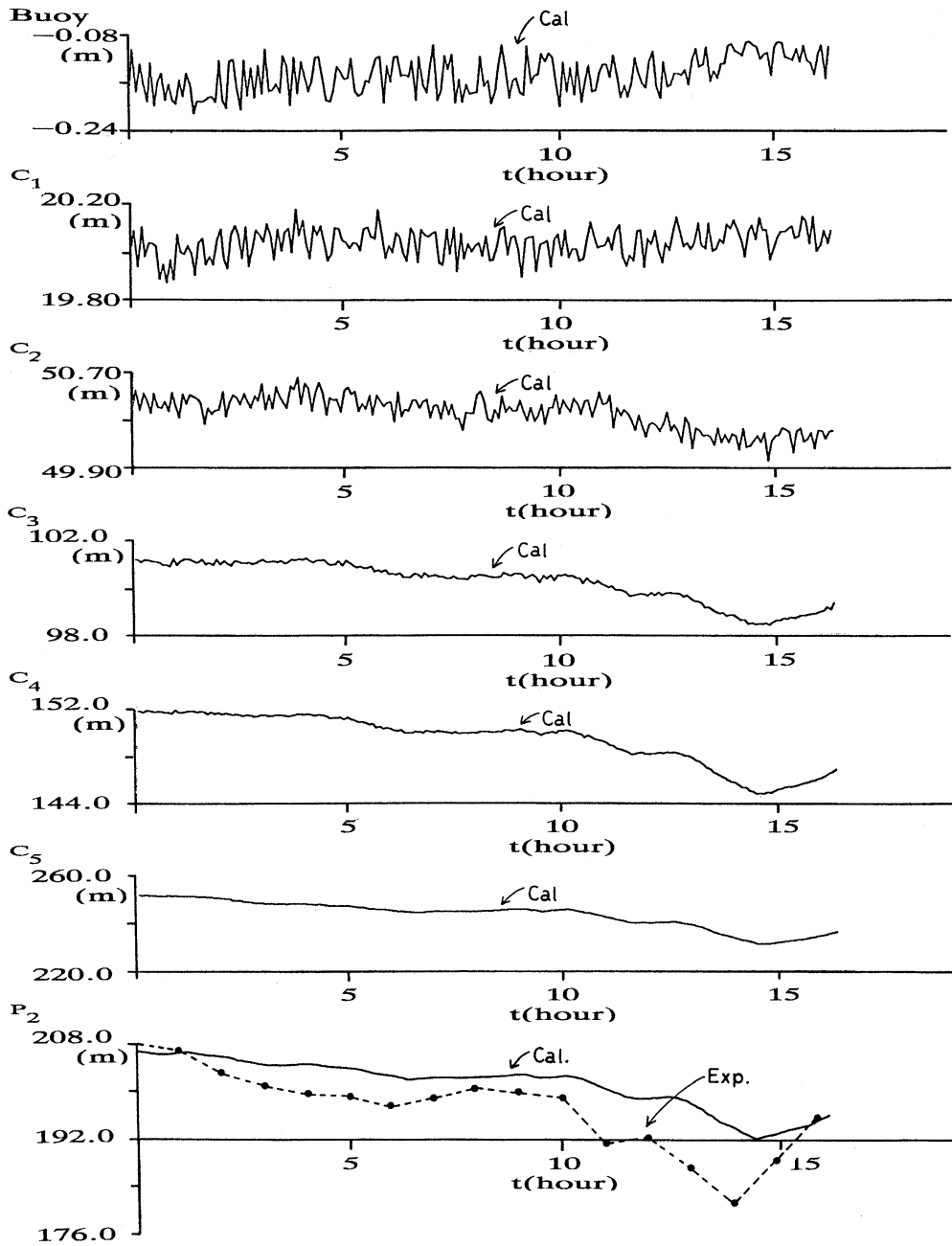


Fig. 12. Vertical displacement of current meters and pressure sensor.

generally the viscous damping is very large in case of the buoy mooring and the ratio does not increase remarkably even at the resonant frequency. The iteration is therefore convergent in usual surface buoy system. In the present buoy

system the drifting velocity was so small, compared with the measured current velocity that we confine ourselves into first approximation. It depends on the research object whether the iterative procedure is continued.

To analyze the data recorded by current meters and thermometers we need vertical displacements of the instruments. As an example, the time series of the vertical displacements during the current oscillation are shown in Fig. 12. Calculations indicate that the vertical displacement of the surface buoy is about 0.1m and that of C_1 is 0.2m. Both are very small. The value of C_3 (16m) is fairly large. When the data collected by thermometers and current meters are analyzed, the vertical displacement of the instruments should be taken into consideration, especially for the lower instruments. We set two pressure sensors, P_1 and P_2 at depths of 105m and 205m (Fig. 3) to measure the vertical displacements, but in the present experiment P_1 did not work well. In Fig. 12 the calculated result (solid line) is compared with the measured value of vertical displacement by pressure sensor P_2 (black circles and broken line). Both are in good agreement.

4. Conclusions

A deep sea surface buoy system for ocean mixed layer experiments was designed and manufactured. On-site experiments were carried out and the accuracy of collected data was discussed using numerical simulations. The main conclusions are as follows:

1. The drifting velocity of surface buoy system induced by the current oscillation is much smaller than the current velocity.
2. The motion velocities of the buoy system induced by surface waves are large and the accuracy of current measurement is questionable in a severe storm unless a vector-average type current meter is used.
3. From conclusions 1 and 2, the accuracy of the current data with the surface buoy system would be much improved by using a vector-average type current meter and can be compared with that of the submerged buoy system.
4. The accuracy of calculations using the Lumped Mass Method was confirmed by experiments.

Acknowledgments

The authors thank the crews of the Hakuho Maru of the Ocean Research Institute of Tokyo University, the Keiten Maru and the Kagoshima Maru of Kagoshima University for their contributions in the on-site experiments and the staff of the Japan Meteorological Agency for providing us the valuable data of meteorological buoys around Japan. The authors also express their appreciation to Miss Aki YOSHIDA for preparing the manuscript.

References

- CLAY, P.R. (1983): The LOTUS discus mooring. Woods Hole Oceanogr. Inst. Contr. No. 5354, 1-6.
- EKMANN, V.W. (1905): On the influence of the earth's rotation on ocean currents. Ark. F. Math. Astr. Och. Fysik.
- KOTERAYAMA, W., S. MIZUNO and H. MITSUYASU (1986): Preliminary design of deep-sea surface buoy system for ocean mixed layer experiments. La mer, 24, 139-149.